



HAL
open science

Speed based optimal power control in small cell networks

Veeraruna Kavitha, Manu K Gupta, Véronique Capdevielle, Rahul Kishor M.,
Majed Haddad

► **To cite this version:**

Veeraruna Kavitha, Manu K Gupta, Véronique Capdevielle, Rahul Kishor M., Majed Haddad. Speed based optimal power control in small cell networks. *Computer Communications*, 2019, 142-143, pp.48 - 61. 10.1016/j.comcom.2019.04.009 . hal-03484670

HAL Id: hal-03484670

<https://hal.science/hal-03484670>

Submitted on 17 Dec 2021

HAL is a multi-disciplinary open access archive for the deposit and dissemination of scientific research documents, whether they are published or not. The documents may come from teaching and research institutions in France or abroad, or from public or private research centers.

L'archive ouverte pluridisciplinaire **HAL**, est destinée au dépôt et à la diffusion de documents scientifiques de niveau recherche, publiés ou non, émanant des établissements d'enseignement et de recherche français ou étrangers, des laboratoires publics ou privés.



Speed based optimal power control in small cell networks

Veeraruna Kavitha^{a,*}, Manu K. Gupta^b, Véronique Capdevielle^c, Rahul Kishor M.^a,
Majed Haddad^d

^a Industrial Engineering and Operations Research, IIT Bombay, Mumbai, India

^b Singapore University of Technology and Design, Singapore

^c Nokia, France

^d University of Avignon, France

ARTICLE INFO

Keywords:

Small cell networks
Mobility
Power control
Drop probability
Constrained optimization

ABSTRACT

Small cell networks promise good quality of service (QoS) even for cell edge users, however pose challenges to cater to the high-speed users. The major difficulty being that of frequent handovers and the corresponding handover losses, which significantly depend upon the speed of the user. It was shown previously that the optimal cell size increases with speed. Thus, in scenarios with diverse users (speeds spanning over large ranges), it would be inefficient to serve all users using common cell radius and it is practically infeasible to design different cell sizes for different speeds. Alternatively, we propose to allocate power to a user based on its speed, e.g., higher power virtually increases the cell size. We solve well known Hamiltonian Jacobi equations under certain assumptions to obtain a power law, optimal for load factor and busy probability, for any given average power constraint and cell size. The optimal power control turns out to be linear in speed. We build a system level simulator for small cell network, using elaborate Monte-Carlo simulations, and show that the performance of the system improves significantly with linear power law. The power law is tested even for the cases, for which the system does not satisfy the assumptions required by the theory. For example, the linear power law has significant improvement in comparison with the 'equal power' system, even in presence of time varying and random interference. We observe good improvement in almost all cases with improvements up to 89% for certain configurations.

1. Introduction

Since the advent of smartphones, mobile networks are witnessing an exponential traffic growth. Cisco has recently predicted 11-fold increase in the global mobile data traffic between 2015 and 2020 [1], while Qualcomm has forecasted an astounding 1000x increase in mobile data traffic in near future [2]. The increased traffic creates new challenges for service provider in various aspects, for example, mobility management [3]. To cater to the increasing traffic demands, cellular networks are transformed into heterogeneous networks (HetNets), by deploying additional small cells (pico cells, femto cells, metro cells, etc.) along with the existing macro cells [4,5]. Sometimes, small base stations (BSs) are installed in high traffic sub-regions to share the load of the macro BS. Major streets (high ways) are one such example sub regions, which often carry heavy traffic. Proposals are made to install small BSs on the lamp posts along the side of major streets/high ways (e.g., [6]).

Mobility management raises various novel research questions for short radius cells, more so when they cater to high speed users. As the cell size decreases, the handover rate critically increases especially for high or medium speed users which will increase the rate of call

drops [7]. Any handover is dropped if the entering new cell does not have a free server. Thus, the drop rate increases with the frequency of handovers. On the other hand, with reduced cell radius, one can serve even the cell edge users with good service rate.

This trade-off (good service rates versus handover loss) is studied in [8] and optimal cell size for appropriate performance measure (e.g., expected service time, load factor and drop or busy probability, etc.) is obtained. It was concluded that the optimal cell size for higher velocity users is larger. However, it would be a practically infeasible procedure to vary the physical cell size based on speed. 3GPP has proposed to offset the received signal power from various BSs to the user (under consideration) using a cell selection bias (CSB), before selecting the serving BS of the user. With CSB, one may not always select the BS with the strongest received power. The main idea is to favour the handover (HO) of high mobility users towards macro cells, while low or medium mobility users are offloaded to small cells. But this is a coarse (small or macro BS) control, which may not improve the performance significantly.

* Corresponding author.

E-mail address: vkavitha@iitb.ac.in (V. Kavitha).

We propose to allocate power to the users based on their speed, which makes it possible to have a fine control. The higher power virtually increases the cell size: a far away user with higher power can be served at the same transmission rate as a near-by user with an appropriate smaller power (capacity of the far away user increases with higher power) [9]. This work is motivated by above natural phenomenon. One can have as many levels of power allocation as required, enabling finer control. We derive *optimal speed-based power allocation* policies.

The user speed estimates have been recently studied by many researchers in small cell networks [10–12]. These estimates may (or may not) be available with high accuracy. If the estimates are not accurate, one can classify the users into finite number of classes (each class specified by a range of user speeds); allocate same power to all the users in a speed class. We derive a closed form expression for an optimal power control vector, whose components represent the power allocated to different speed classes, subject to a constraint on the average power used. We refer this as *discrete* power law. Alternatively, if the user speed can be estimated accurately, we obtain the optimal power law using Hamilton–Jacobi–Bellman (HJB) equations and Lagrange multipliers as function of user-speed. We refer this as *continuous* power law.

The continuous law turns out to be (affine) linear with user speed. The disparities in the powers allocated to various speeds, increases with the increase in the path-loss factor and (or) the cell size. Further the discrete power law converges to continuous one, as the number of speed classes increases to infinity. The numerical experiments confirm a remarkable improvement in drop probability with optimal power law, in comparison with the case where equal power is allocated to all the users. The performance improves as the number of speed classes increases and best performance is obtained with continuous law. However, a significant improvement is achieved with just *two* user-speed classes.

The optimal power law is derived under the assumption of *zero interference* from other cells due to theoretical tractability. However, we built a system level small cell network simulator (SCNS) to test the performance of optimal power law and we included some test cases with interference. The SCNS is made by emulating cars moving along a straight road (with random speeds), and receiving (random amount of) service from a series of pico towers adjacent to the road. This simulator assumes perfect transmission when one operates below the capacity (at that time and at that position). First, we validate SCNS in order to test the optimal power law. We notice that power law *fails* only when the block/drop probabilities are large (of order 10^{-1}). However, wireless networks seldom operate in such scenarios due to low efficiency.

SCNS is used extensively to test the applicability of the proposed power law. We consider different test cases spanning over various configurations, for example, with a common set of transmission rates, and or with different levels of interference and or with various user speed profiles etc. We notice a significant improvement (most of the cases above 30% and upto 89% in some cases) in performance with linear power law in comparison with the systems that allocate equal power to all users. The improvement is significant even for the test cases that do not satisfy the assumptions required by theory, e.g., test cases considering the influence of interference or non-uniform speeds etc. Even in the presence of interference we noticed good improvement (some cases upto 70%).

Related work: For an excellent survey on power control in wireless networks, readers are referred to [13] and references therein (e.g., [14–19]). Most of the existing algorithms focus on either optimizing the total power spent while maintaining QoS or optimizing the QoS under a power budget constraint. Further refinement on these algorithms are based on speed of the user (e.g., [20–22] are few of them). These algorithms either vary a control parameter or a step size of the adaptive algorithm so that the algorithm is better suited to the user mobility. They explore the convergence issues associated with mobility patterns. While we consider a small cell network with one dimensional users

where: (a) the service rate is adapted based on the received SNR; and hence (b) the rate varies in a periodic fashion as the distance between unidirectional user and the serving BSs changes periodically. Given such a system, we obtain the performance which is sensitive to the speed of the user due to frequent HOs. We come up with the classification of users based on their speed and power control, so as to improve the performance of the overall system which shares resources among all the users. Most of the existing algorithms attempt to overcome the hurdles created by difficult phenomenon such as high speed variations, whereas our fundamental goal is to design optimal systems based on these variations. We achieve this goal by deriving an optimal policy which can either be stored as a lookup table (in case of finite classes) or the formula can be remembered and system can allocate power using this stored information and the estimate of the user speed (in case of continuous power control). Thus this algorithm has negligible overload and one can use this in self organizing networks.

Authors in [8] considered uni-directional users travelling on a straight road, while deriving service from series of BSs. In [8], it is assumed that the rate of communication can be changed continually that too with “maximal” transmission rates (i.e., capacity). This gives “maximal” performance, which is not realistic. We also consider a similar uni-directional user scenario, but for a radically different change in the selection of the transmission rates: communication can happen at one of the N given choices of the transmission rates. At any given time, the rates chosen are less than the “maximal” transmission rate (capacity) at that time.

Parts of this work were presented in [23]. In this paper, we generalized the set of rates and more importantly included the system level simulator. The system should provide sufficiently large choices of transmission rates to obtain significant advantage of power law. The more the choices, the finer is the control and better would be the improvement in performance. In [23], we assumed that system supports N choices and the set of these choices is different for different speeds. In this paper, using the system level simulator, we also include a study with a common (possibly bigger) set of rate choices. We then consider the influence of interference on the performance of the proposed linear law, by comparing it with the system that allocates equal power to all users. We study this comparison using the system level simulator and perform detailed numerical analysis, which includes random and time varying interference patterns resulting from randomly originated and moving users deriving service from the encountered small cell base stations. We observe that the improvement in performance (though reduced once interference is considered), is significant even in the presence of *interference*.

This paper is organized as follows. The system model is described in Section 2, performance measures are derived in Section 3 and the optimal power law is obtained in Section 4. The simulator and the extensive numerical results are described in Sections 5–7. Section 8 concludes the paper.

2. System model

We consider users moving in a fixed direction. The users are moving in one direction (in a one dimensional line $[-D, D]$) and at high speeds, which vary negligibly during the call. One such example (see Fig. 1) is when user, driving in a car, derives its service from portable BSs which are installed on street infrastructure (like lamp posts). The distance between successive BSs is $2L$. The users can move in one of the two directions with equal probability, i.e., with half probability. We assume symmetry in both the directions and hence any performance (e.g., busy probability, drop probability etc.), conditioned on the direction of the user, will be same for both the directions. Thus, without loss of generality we only consider users moving from *left to right*. We assume the channel to be weakly time-varying. In particular, we assume that the optimal power allocation is achieved before significant channel variations, as is customarily assumed in all power control schemes.

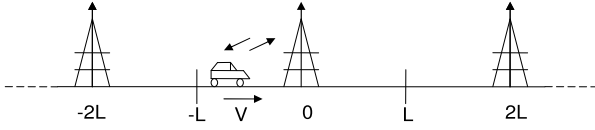


Fig. 1. User moving in a car while deriving service.

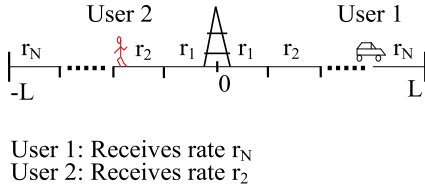


Fig. 2. Rate partitioning and user's movement.

The user moves with speed V , which is independent and identically distributed (IID) across various users. We assume uniform arrivals in the system. In small cell networks, the (adjacent) BSs are reasonably close and hence one has to design carefully with sufficient reuse factor to avail the advantages of small BS separations. In this work, we indeed assume this is the case for theoretical results, i.e., we assume no interference from the other cells. Many other techniques like interference cancellation, beam forming etc. are used to effectively mitigate interference. Alternatively one can assume interference to be constant and our results follow under such assumption on interference. This assumption is valid when one gets interference from large number of sources. In the last section of the paper, we present numerical results considering *interference*. We observe that the performance of the optimal policies, derived in this paper, is remarkable even in the presence of interference.

Rate Regions: The cell is divided into $2N$ disjoint segments (depending upon distance from BS¹) and users within a segment are served with the same transmission rate. Let $\{\mathcal{A}_n\}_{n \in \mathcal{N}}$ represent these segments (see Fig. 2):

$$\begin{aligned} \mathcal{A}_n &:= [\phi_{n-1}L, \phi_n L] 1_{\{n>0\}} + [\phi_n L, \phi_{(n+1)}L] 1_{\{n<0\}}, \\ \mathcal{N} &:= \{-N, \dots, -1, 1, \dots, N\}, \end{aligned} \quad (1)$$

where the coefficients $\{\phi_n\}$ determine the partition of the cell, with $\phi_n = -\phi_{-n}$ for all n . Segments $\mathcal{A}_n, \mathcal{A}_{-n}$ placed at the same distance on either side of BS (Fig. 2) are served with common rate r_n and these common rates decrease as the distance from BS increases. Let $\mathcal{R} := \{r_1, \dots, r_N\}$ (decreasing set) represent the ensemble of all possible transmission rates. The service rate changes once the user moves from one region to another. We consider $\phi_0 := 0$ for notational simplicity, and there is actually no change in rate when users move from \mathcal{A}_{-1} to \mathcal{A}_1 .

Arrivals: There are two types of arrivals: (1) arrivals from external world (represented by subscript e and this subscript is used only when there is ambiguity) modelled as Poisson arrivals with parameter λ ; (2) HO arrivals (subscript h) modelled again as Poisson² arrivals is the sub-stream of external arrivals whose service is not completed in the previous cell. Rate of arrivals into the cell of interest $[-L, L]$ (referred as cell 0) depends upon the cell dimension L and this is shown by either λ_L (for external arrivals) or $\lambda_{h;L}$ (for HO arrivals). For external arrivals, we assume³ $\lambda_L = \lambda L$ while $\lambda_{h;L}$ will be derived in later sections. Every

¹ In small cell networks (transmission at small distances), distance based propagation losses would be sufficient for deciding the theoretical rate limits as well as the practical transmission rates.

² This is a commonly made assumption, see [24,25].

³ If the arrivals in the entire line segment $[-D, D]$ occur at rate λ' those in segment $[-L, L]$ occur at a smaller rate $\lambda_L = \lambda' \text{Prob}(\text{arrival in } [-L, L])$. For the special case of uniform arrivals (i.e., arrivals landing uniformly in $[-D, D]$) $\lambda_L = \lambda L$.

arrival brings along with it the marks (Φ, S) , where $\Phi \in \mathcal{N}$ is the position of arrival with distribution $\Pi := \{\pi_n\}_n$ and S , the number of bytes to be transmitted, is exponentially distributed, i.e., $S \sim \mu \exp^{-\mu t}$ for some $\mu > 0$.

Resources: A cell can attend K parallel calls. The power per transmission P can depend upon the speed of the user and we obtain the optimal power function given an average power constraint.

Set of transmission rates \mathcal{R} : With speed based power control, there would be significant variations in the received power. One can consider different set of rates for different speeds to design an efficient system. Alternatively, one can consider a common set of supported rates which is sufficiently big and choose one among them based on the received signal. First alternative is discussed below, while the other scenario is explored in Section 7. As of now, we assume that the system has predefined rate regions which are common for all the speeds/transmit powers. The (common) rate supported in any given rate region depends upon the transmit power and the farthest point of the region. The capacity of the farthest point provides the best possible rate.

We use the following low SNR approximation of the theoretical (capacity) rate⁴:

$$r(d) := P \left(1_{\{d \leq d_0\}} + r_0 |d|^{-\beta} 1_{\{d > d_0\}} \right) \text{ with } r_0 = d_0^\beta. \quad (2)$$

Here, $r(d)$ is the rate at distance d , d_0 is a small lossless distance⁵ while β is the propagation co-efficient. The farthest user of \mathcal{A}_n , will be at distance $|\phi_n|L$. Hence the maximal transmission rate, that can be allocated, equals

$$r_n = r(\phi_n L) = r_0 P L^{-\beta} |\phi_n|^{-\beta}. \quad (3)$$

Remark: Alternatively, if the system under consideration can design modulation and or channel coding schemes so as to achieve (almost) ν percent of the theoretical rates where $\nu < 1$ is a fixed coefficient, then again the above rate structure is applicable (after absorbing ν into r_0 of (3)).

Handovers: When the user reaches the boundary ($|x| = L$) the call is handed over to the neighbouring cell (if the call is not completed and free servers are available in the new cell).

Information to initiate HO: Every new connection requires s_h extra bytes to be exchanged to initiate it. The effect of these bytes (on the system performance) for a new call will be negligible (as it would be once), however one needs to consider their effect on HO calls. These bytes are usually very small in proportion to the actual information to be transmitted, i.e., $s_h \ll S$ with probability close to one. In particular we assume that $\mu s_h \ll 1$. We also assume that s_h bytes are exchanged with probability very close to one (actually w.p.1), while user is in the last region r_{-N} .

Notations: We denote the transpose by t . Calligraphic letters represent mostly represent sets (e.g., \mathcal{N} — set of segment numbers, \mathcal{R} — set of all possible transmission rates, \mathcal{A}_n — rate region n). The contents inside two flower brackets represent either a set or an ordered tuple (as according to convenience); for example $\{r_n\}_n$ represents the set \mathcal{R} while $\{\pi_n\}_n$ represents the ordered tuple Π . Lower case letters represent time index (k) or the segment index (n).

Upper case letters represent system parameters. For example, D — dimension of macro cell, L — dimension of small cell, P — Power per transmission, K — Number of servers, N — Total number of possible transmission rates (number of elements in \mathcal{R}), $\Pi = \{\pi_n\}_n = \{\text{Prob}(\text{Arrival in segment } n)\}_n$ — Vector of arrival probabilities etc. Upper case letter can also represent random variables (V — Velocity, S — number of bytes to be transmitted etc.).

⁴ For unit noise variance, capacity equals $\log(1 + SNR)$, where signal to noise ratio $SNR = PA$ and attenuation $A = 1_{\{d \leq d_0\}} + (d/d_0)^{-\beta} 1_{\{d > d_0\}}$. For low SNRs, $\log(1 + SNR) \approx SNR$ and hence capacity equals PA .

⁵ Typically d_0 is small and in this paper we consider optimizing over cell sizes $L > d_0 N$. That is, we always consider distances $d > d_0$ and hence use the simpler formula $r(d) = r_0 P d^{-\beta}$.

3. User speed dependent performance measures

In this section we derive the performance metrics (e.g., load factor, busy probability, drop probability etc.), which capture the trade off between HO losses and the service quality, for a given user speed profile. We eventually conclude this section by showing that the optimizers of load factor and busy probability are the same.

We consider non elastic traffic which comprises of users demanding immediate service. These users (e.g., voice calls) drop the call if it is not picked up immediately, i.e., if all the K servers are busy (see [8,26]). The probability that a call is not picked up immediately is called the *Busy probability* P_{Busy} and the probability that a call that was picked up is ever dropped before completing its service is called the *Drop probability* P_{Drop} . The former is the probability that an incoming call is not picked-up, while the later is the probability that, a call that was picked-up, is dropped before service completion. Both these performance metrics depend upon HOs as well as the average service time and hence capture the required trade-off.

In this paper we work with metrics proportional to P_{Busy} , to be specific with load factor ρ (equation (9) derived in later sections). *One can obtain P_{Drop} as in [8] and show that it can be approximately optimized by minimizing the load factor, but we omit this discussion here. Similarly in [8], it is shown (under certain conditions) that the expected waiting time of an elastic user (a user who can wait for its turn but demands high quality of transmission) can be optimized by minimizing the load factor. We expect similar results to hold even in this case. In all, we optimize the load factor ρ .*

Without loss of generality we consider cell 0, $[-L, L]$. Let ψ_n represent the probability that a call originated in rate segment n , \mathcal{A}_n , is completed before reaching boundary $\{L\}$ (one element set). The user is served at rate r_n and hence a total of $(L/N)(1/V)r_n$ bytes are transferred before it crosses \mathcal{A}_n and then served at rate r_{n+1} and so on till it reaches the boundary point L . Total number of bytes transferred during this transit equal $\sum_{m=n}^N r_m L/(NV)$ and so the user will complete its call (i.e., transfer of S (exponential) bytes of information) before leaving the cell with probability (conditioning on V):

$$\psi_n = Prob\left(S < \frac{L}{NV} \sum_{m=n}^N r_m\right) = 1 - E\left[e^{-\frac{\mu L \sum_{m=n}^N r_m}{NV}}\right]. \quad (4)$$

In general it is difficult to obtain the above Laplace transform and hence ψ_n . For example, when V is uniformly distributed. However, one can obtain a good approximation if we assume, $V_{min} \leq V \leq V_{max}$, with V_{max} close to V_{min} and both away from 0. When the high speed users are partitioned to a large number of classes, each class will satisfy the above assumption. Further when μ is small (large jobs) and/or V_{min} is large (as with high speed users of this paper) one can use the approximation, $e^{-x} \approx 1 - x$, and then

$$\psi_n \approx \frac{\mu L \sum_{m=n}^N r_m}{N} E[1/V]. \quad (5)$$

On the other hand, one can approximate $1 - \psi_n$ directly with 1 as ψ_n in (5) is very small in comparison with 1. Let $P_{e,ho}$ ($P_{h,ho}$) represent the probability that a new or external (handover) call is handed over (again) to the neighbouring cell. Note that we are modelling the HOs also as Poisson arrivals. A new call can arrive in any segment \mathcal{A}_n with probability π_n while a HO call always occur at $-L$, i.e., in rate region \mathcal{A}_{-N} (calls are from left to right). Any new arrival (same is the case with HO call) is handed over to the next cell if the call is not completed in the current cell, or if its message S bytes are not transferred completely before the user reaches the cell edge. Finally by unconditioning (w.r.t. the event of arrival being in \mathcal{A}_n) we have,

$$P_{e,ho} = 1 - \sum_{n=-N}^N \pi_n \psi_n \approx 1 - PL^{1-\beta} E[1/V] C_{e,ho} \quad (6)$$

with $C_{e,ho} := \frac{\mu}{N} r_0 \sum_{n=-N}^N \pi_n \sum_{m=n}^N |\phi_m|^{-\beta}$

is an appropriate constant and is obtained by substituting r_n from (3). *Every HO call needs exchange of extra s_h control bytes and an HO call arrives only in \mathcal{A}_{-N} . Thus using similar logic ($C_{h,ho}$ is another constant like $C_{e,ho}$), $P_{h,ho} = 1 - \psi_{-N,h}$ and so:*

$$P_{h,ho} = 1 - Prob\left(S + s_h < \frac{L}{NV} \sum_{m=-N}^N r_m\right) \approx 1 - (C_{h,ho} PL^{1-\beta} E[1/V] - \mu s_h) \quad \text{with}$$

$$C_{h,ho} := \frac{\mu}{N} r_0 \sum_{n=-N}^N |\phi_n|^{-\beta}. \quad (7)$$

3.1. Expected service time

This expected service time is the expected amount of time for which a user is served in a cell. Let b_n represent the expected time for which the service is received in cell 0, given the call is originated in region \mathcal{A}_n . When *high speed users travel in small cells*, with a very high probability a call is not completed in one cell. Hence one can approximate b_n with the time taken to reach the boundary:

$$b_n \approx \sum_{k \geq n} (\phi_{k+1} - \phi_k) LE \left[\frac{1}{V} \right] = L (\phi_N - \phi_n) E \left[\frac{1}{V} \right].$$

Recall that $\phi_n = -\phi_{-n}$. The service time of a new call (b_e) and that of a handed over call (b_h) on average equals (by unconditioning)⁶:

$$b_e = \sum_{i=-N}^N b_n \pi_n = C_{b,e} LE[1/V], \quad C_{b,e} := \sum_{n=-N}^N \pi_n (\phi_N - \phi_n)$$

$$b_h = b_{-N} = C_{b,h} LE[1/V], \quad C_{b,h} := 2. \quad (8)$$

The expectation in $E[1/V]$ is with respect to the distribution of the user speeds. However, the corresponding distribution in b_h (the expected service time for HO users) is the speed distribution of the HO users, which may not be the same as that of the new users. The higher speed users are handed over more frequently than the lower speed ones. So, the distribution of the HO user velocities can be different. In [8, Appendix B], it is shown that the HO user speed distribution converges to new-user speed distribution as the cell size reduces to zero, when the new-user speed distribution is uniform. *In exactly similar lines one can show the same result for any arbitrary new-speed distribution, when it has a density. Thus we approximate the HO user speed distribution with the new-user speed distribution.* That is, we approximate the distribution of V in the expression of b_h with that of the user speed of the new call. Further and more importantly, the accuracy of this approximation increases as the difference $(V_{max} - V_{min})$ decreases. Or equivalently the approximation is accurate, when the number of velocity based user classes, considered in Section 4, increases.

Performance metrics obtained in the remaining part of this section, Section 3, are derived in similar way as in [8,26]. These derivations are obtained using the stochastic equivalence of calls going out of and coming into cell 0 (details are in [8,26]). We present the derivations briefly and more details can be found in the two papers. These results are useful in deriving optimal power law in Section 4.

3.2. HO arrival rate

We obtain the rate, $\lambda_{h:L}$, at which HOs occur. Let λ_L represent the fraction of the new calls that arrive in the cell of interest $[-L, L]$ which equals λL for uniform arrivals (for appropriate $\lambda > 0$). A fraction of the new arrivals as well as HO calls get converted (again) to HO calls. The calls that have not finished their service before reaching

⁶ The time taken for exchange of s_h HO bytes has to be included in the time of the cell utilized by the user and hence the (HO) service time b_h . However, the rate of HOs is high and we are approximating b_h by the average time taken to traverse the entire cell, b_h does not change with s_h .

the boundary are exactly this fraction, whose value is given by $P_{e,ho}$ and $P_{h,ho}$ respectively for new arrivals and the HO calls. By memory less nature of S (the bytes to be transferred), we have a stochastic equivalence between the calls entering and leaving the cell (see [8,26]). Basically the fraction of new arrivals that get converted to HO calls would be $\lambda_L P_{e,ho}$ and the number of HO calls that get converted to HO calls (again) would be $\lambda_{h,L} P_{h,ho}$ and the sum of these two should equal the rate of HO arrivals $\lambda_{h,L}$ because : (a) either of the former calls require same amount/distribution of job to be done (remaining S is again exponentially distributed); and (b) either of these calls will need to communicate using extra s_h bytes to affect the transfer of call to the entering cell. Using this, $\lambda_{h,L}$ satisfies the fixed point equation, $\lambda_{h,L} = \lambda_L P_{e,ho} + \lambda_{h,L} P_{h,ho}$. Hence, from Eqs. (6), (7)

$$\lambda_{h,L} = \frac{\lambda_L P_{e,ho}}{1 - P_{h,ho}} = \lambda_L \frac{1 - PL^{1-\beta} E[1/V] C_{e,ho}}{PL^{1-\beta} E[1/V] C_{h,ho} - \mu s_h}.$$

3.3. Overall expected service time

(On considering both HO and new arrivals) equals (see (8)),

$$\bar{b} = \left(\frac{\lambda_L}{\lambda_L + \lambda_{h,L}} b_e + \frac{\lambda_{h,L}}{\lambda_L + \lambda_{h,L}} b_h \right).$$

By ergodicity, the probability that a given call is new, equals the ratio of the arrival rate of new or external calls and the arrival rate of all the calls and hence the above result.

3.4. Load factor

The product of the average service time and the arrival rate gives the rate at which the overall load is arriving into the system and this product divided by the number of servers is called load factor, which is given by:

$$\rho = (\lambda_L + \lambda_{h,L}) \bar{b} / K.$$

On simplification,

$$\rho = \frac{\lambda L^2 E[1/V]}{K} \left(C_{b,e} + C_{b,h} \frac{1 - PL^{1-\beta} E[1/V] C_{e,ho}}{PL^{1-\beta} E[1/V] C_{h,ho} - \mu s_h} \right). \quad (9)$$

3.5. Busy probability

A small cell catering to non elastic traffic can be modelled by an M/G/K/K queue (as in [8]). By Erlang's loss formula, busy probability

$$P_{Busy} = \frac{\rho^K / K!}{\sum_{k=0}^K \rho^k / k!}. \quad (10)$$

Thus from above, the busy probability depends upon L only via ρ and both are differentiable in L . By differentiating twice one can immediately obtain the following result (see [8, Theorem 5] for similar details).

Lemma 1. *Optimizers of ρ and P_{Busy} are same, i.e.,*

$$L_\rho^* := \arg \inf_L \rho = \arg \inf_L P_{Busy}(L) =: L_{P_{Busy}}^*. \quad \square$$

By Lemma 1, the cell size optimizing P_{Busy} is the same as that optimizing the load factor. In a similar way the power control affects busy probability only via the load factor ρ . Hence we optimize load factor (ρ) in subsequent sections.

4. Optimal power law

In this section, we derive optimal power law for the given cell size L and power constraint \bar{P} . Subsequent sections discuss the optimal power law for finite and infinite number of user classes.

4.1. Finite number of user classes

The users are divided into different classes based on their speeds. Divide the (speed) interval $[V_{min}, V_{max}]$ into I disjoint intervals $\{I_i\}_{i \leq I}$ and classify users into one of the I classes based on their speed. From (9), load factor ρ depends upon the user speed profile only via $E[1/V]$ and so we are interested in the conditional expectation

$$Y_i := E \left[\frac{1}{V} \middle| V \in I_i \right].$$

Let $p_i := \text{Prob}(V \in I_i)$ represent the probability of class i and P_i is the transmit power allocated to class i .

HO rates of the different user classes can be calculated using earlier logic:

$$\lambda_{h,L,i} = \lambda_{L,i} \frac{P_{e,ho,i}}{1 - P_{h,ho,i}} = \lambda L p_i \frac{1 - P_i L^{1-\beta} Y_i C_{e,ho}}{P_i L^{1-\beta} Y_i C_{h,ho} - \mu s_h}.$$

Similarly the expected service time for different user classes can be obtained and then the overall load factor ρ simplifies⁷:

$$\begin{aligned} \rho(L, \mathbf{P}) &= \frac{1}{K} \left(\lambda_L b_e + \sum_i \lambda_{h,L,i} b_{h,i} \right) \\ &= \frac{\lambda L^2}{K} \sum_i p_i Y_i \left(C_{b,e} + C_{b,h} \frac{1 - \delta_i C_{e,ho}}{\delta_i C_{h,ho} - \mu s_h} \right) \end{aligned} \quad (11)$$

where $\delta_i := P_i Y_i L^{1-\beta}$. We are interested in power control $\mathbf{P} := \{P_1, \dots, P_I\}$ which minimizes ρ while the average power satisfies following constraint:

$$\sum_i p_i P_i \leq \bar{P}.$$

Assuming that \bar{P} is sufficiently large to ensure useful communication (see Appendix A), one can solve above optimization problem and we obtain:

Theorem 1. *Assume $C_{h,ho} - \mu s_h C_{e,ho} > 0$ and assume that the following matrix is positive definite,*

$$P_V := \begin{bmatrix} p_1 + \frac{p_1^2}{P_1} & \frac{p_1 p_2}{P_1} & \dots & \frac{p_1 p_{I-1}}{P_1} \\ \frac{p_1 p_2}{P_1} & p_2 + \frac{p_2^2}{P_1} & \dots & \frac{p_2 p_{I-1}}{P_1} \\ \vdots & \vdots & \ddots & \vdots \\ \frac{p_1 p_{I-1}}{P_1} & \frac{p_{I-1} p_2}{P_1} & \dots & p_{I-1} + \frac{p_{I-1}^2}{P_1} \end{bmatrix} > 0.$$

Then, the power control that minimizes ρ , given by (11), while satisfying the average power constraint equals:

$$P_i^*(L; \bar{P}) = \bar{P} + \frac{\mu s_h L^{\beta-1}}{C_{h,ho}} \left(\frac{1}{Y_i} - \sum_j p_j \frac{1}{Y_j} \right), \quad Y_i := E \left[\frac{1}{V} \middle| V \in I_i \right]. \quad (12)$$

Proof: is provided in Appendix B. \square

From (6)–(7) $C_{h,ho} \geq C_{e,ho}$ and from our earlier assumptions, $\mu s_h \ll 1$. So, the first assumption would be trivially satisfied. The second assumption is often satisfied, for example when users are classified into I uniform classes, i.e., when

$$I_i = V_{min} + \left[\frac{i-1}{I}, \frac{i}{I} \right] (V_{max} - V_{min}) \quad \text{and so } p_i = \frac{1}{I} \quad \forall i.$$

We obtain the following interesting properties of the optimal power division (from (12)): (1) allocated power increases with the speed range

⁷ Load factor ρ equals the product of total average arrival rate ($\bar{\lambda} := \lambda_L + \sum_i \lambda_{h,L,i}$) and average service time divided by K . An arrival turns out to be a new arrival with probability $\lambda_L / \bar{\lambda}$, it turns out to be an HO arrival of class i with probability $\lambda_{h,L,i} / \bar{\lambda}$ and so average service time equals $(\lambda_L b_e + \sum_i \lambda_{h,L,i} b_{h,i}) / \bar{\lambda}$.

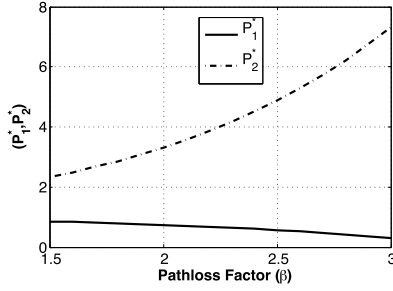


Fig. 3. Optimal power control for two user classes.

of users in a class (users with lower Y_i get higher power), which in turn implies an increased virtual cell; (2) the disparity in the allocated powers between different classes increases with cell size, the disparity in speeds and the path-loss factor. Thus from (12) in a medium with large path losses, one needs to allocate larger power to high speed users in order to improve the overall system performance. Intuitively otherwise, large speed users hold on to the system resources for longer time periods which can deteriorate the performance of the low speed users. And the same applies to the case when the system has to support wide range of user speeds ($V_{max} - V_{min}$).

4.2. Continuous optimal power law

When one has an accurate estimate of the velocity, it might be optimal to do finer power control, i.e., transmit power is varied continually based on the precise value of velocity. Further, as mentioned in the previous sections, the modelling inaccuracies (while obtaining HO rates, HO velocity distribution etc.) mitigate as the number of classes increase. In this continuous case, we expect to model more accurately.

We assume that user velocity is a continuous random variable with density $p_V(v)$ and with support in the range $[V_{min}, V_{max}]$ for some $0 < V_{min} < V_{max} < \infty$. For example for uniform case, $p_V(v) \equiv 1/(V_{max} - V_{min})$.

We obtain an optimal power law, which is a function of velocity v and optimizes the load factor ρ . By power law we meant a function $P(\cdot)$ which maps velocity v to a positive real number, that represents the power allocated to user travelling with speed v . We are only interested in those functions, whose average is constrained by \bar{P} , i.e., we are interested in policies, $\{P(\cdot)\}$, that satisfy:

$$\int_{V_{min}}^{V_{max}} P(v)p_V(v)dv \leq \bar{P}.$$

Let B represent the random service time (the time for which the cell resources are utilized by the user). The conditional average service times $b_e(v)$, $b_h(v)$, the probabilities of service not getting completed $P_{e,ho}(v)$, $P_{h,ho}(v)$ and the HO rates $\lambda_{h,L}(v)$ can be computed by conditioning on user velocity V as in the previous section. These expressions depend upon the power policy $P(\cdot)$. It is easy to see that these conditional expressions will be same as in the previous section except that $Y_v = E[1/V|V \in (v-dv, v+dv)]$ (conditioned that V is in an infinitesimal interval around v) has to be replaced by $1/v$, i.e., for example:

$$b_e(v) = \frac{C_{b,e}L}{v}, \quad P_{e,ho}(v) = 1 - \frac{P(v)L^{1-\beta}C_{e,ho}}{v}$$

$$b_h(v) = \frac{C_{b,h}L}{v}, \quad P_{h,ho}(v) = 1 - \frac{P(v)L^{1-\beta}C_{h,ho}}{v} + \mu s_h.$$

Overall arrival rate

By conditioning and un-conditioning on velocity V , the overall arrival rate including the HOs, equals (E is the expectation with respect to V):

$$\bar{\lambda} = E[\lambda_L(V) + \lambda_{h,L}(V)] = \lambda LE \left[1 + \frac{P_{e,ho}(V)}{1 - P_{h,ho}(V)} \right]. \quad (13)$$

Parameter settings

$$N = 3, \quad d_0 = 10, \quad r_0 = .4d_0^\beta, \quad K = 60, \quad \lambda = 0.7, \quad s_h = 0.4, \quad \mu = 0.2, \quad (\Upsilon_1, \Upsilon_2) = (.05, .02), \quad \bar{P} = 1, \quad L = 70$$

$$(p_1, p_2) = (0.9, 0.1),$$

4.2.1. Average of the overall service time B

The expected value of B is obtained in Appendix C and it equals:

$$\bar{b} = \frac{E \left[b_e(V) + b_h(V) \frac{P_{e,ho}(V)}{1 - P_{h,ho}(V)} \right]}{E \left[1 + \frac{P_{e,ho}(V)}{1 - P_{h,ho}(V)} \right]} \quad (14)$$

$$= \frac{L}{E \left[1 + \frac{P_{e,ho}(V)}{1 - P_{h,ho}(V)} \right]} \int_{V_{min}}^{V_{max}} \left(C_{b,e} + C_{b,h} \frac{1 - \frac{P(v)L^{1-\beta}C_{e,ho}}{v}}{\frac{P(v)L^{1-\beta}C_{h,ho}}{v} - \mu s_h} \right) \frac{p_V(v)}{v} dv.$$

And so the load factor

$$\rho = \frac{\lambda L^2}{K} \int_{V_{min}}^{V_{max}} \left(C_{b,e} + C_{b,h} \frac{1 - \frac{P(v)C_{e,ho}}{L^{\beta-1}v}}{\frac{P(v)C_{h,ho}}{L^{\beta-1}v} - \mu s_h} \right) \frac{p_V(v)}{v} dv. \quad (15)$$

We are interested in power law $\{P^*(\cdot)\}$ which minimizes the load factor ρ under the average power constraint. One can rewrite:

$$\frac{1 - \frac{P(v)C_{e,ho}}{L^{\beta-1}v}}{\frac{P(v)C_{h,ho}}{L^{\beta-1}v} - \mu s_h} = -\frac{C_{e,ho}}{C_{h,ho}} + \frac{1 - \mu s_h \frac{C_{e,ho}}{C_{h,ho}}}{\frac{P(v)C_{h,ho}}{L^{\beta-1}v} - \mu s_h}.$$

We again assume, $C_{e,ho}\mu s_h < C_{h,ho}$, this makes the numerator of the second factor positive and after leaving out the constants the optimal power law is given by:

$$P^*(\cdot) = \arg \inf_{P(\cdot)} \left(\int_{V_{min}}^{V_{max}} \frac{1}{P(v)C_{h,ho} - vL^{\beta-1}\mu s_h} p_V(v)dv \right)$$

$$\text{subject to } \int_{V_{min}}^{V_{max}} p_V(v)P(v) \leq \bar{P}. \quad (16)$$

With ρ representing the Lagrange multiplier we minimize:

$$\int_{V_{min}}^{V_{max}} \left(\frac{1}{P(v)C_{h,ho} - vL^{\beta-1}\mu s_h} - \rho(P(v) - \bar{P}) \right) p_V(v)dv.$$

This is (exactly resembles) a state independent optimal control problem, for any given ρ and can be solved using Hamilton–Jacobi–Bellman (HJB) equation (see for e.g., [27,28]):

$$\frac{dU}{dv} = p_V(v) \inf_P \left\{ \frac{1}{C_{h,ho}P - \mu s_h L^{\beta-1}v} - \rho P \right\} \quad (17)$$

where U , the value function, is given by:

$$U(v) := \inf_{P(\cdot)} \int_v^{V_{max}} \left[\frac{1}{P(v)C_{h,ho} - vL^{\beta-1}\mu s_h} - \rho P(v) \right] p_V(v)dv.$$

The value function U satisfies the HJB equation (17) when it is continuously differentiable (e.g., [27,28]) and we will see that this indeed is the case. The optimal control $P^*(\cdot)$ equals the minimizer of the optimization in the right hand side of the HJB equation (17) (see for example [27,28]). This can be computed easily for any v and

$$P^*(v) = \frac{1}{C_{h,ho}} \mu s_h L^{\beta-1}v + \sqrt{\frac{1}{C_{h,ho}\rho}}.$$

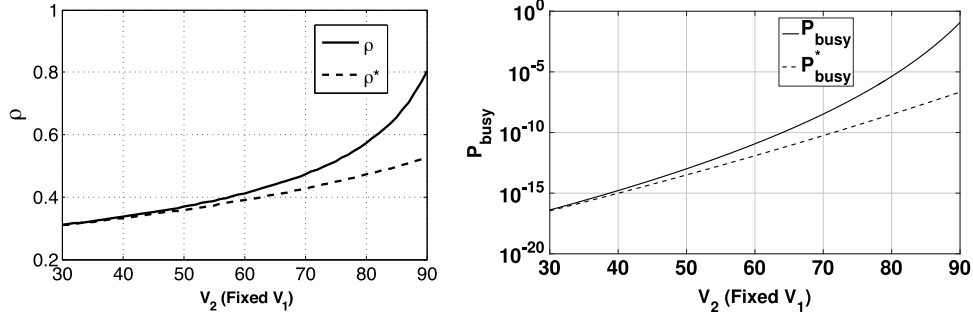


Fig. 4. Performance comparison (load factor and busy probability) with and without optimal power control, as V_2 varies.

The average power equals:

$$\int_{V_{min}}^{V_{max}} P^*(v)p_V(v)dv = \frac{1}{C_{h,ho}} \mu s_h L^{\beta-1} E[V] + \sqrt{\frac{1}{C_{h,ho}\rho}}$$

Equating the above to average power constraint \bar{P} , we obtain the optimal Lagrange multiplier ρ and optimal power law:

Theorem 2. The power function $P^*(\cdot)$ that optimizes ρ given by (15), while satisfying the average power constraint equals:

$$P^*(v) = \bar{P} + \frac{1}{C_{h,ho}} \mu s_h L^{\beta-1} (v - E[V]). \quad (18)$$

Remarks: From (18), we notice that the optimal power law is linear in the speed. In fact even from discrete case (12), it is proportional to $1/Y_i$ which approximately equals a speed $v \in I_i$ if interval I_i is sufficiently thin. This is surprising for us, as we anticipated that the power law will be scaled by factors proportional to path-loss factor β . We reconfirmed using the small cell network simulator built in Section 6 that, the linear power law indeed performs superior in comparison to many other functions. We compared linear power law (18) with power functions that are square or square root of the velocity ($P(v) \propto v^2$ or \sqrt{v}) or functions such that ($P(v) \propto v^\beta$ or $1/v^\beta$) etc., and observed that the former provides the best performance. However the coefficients of the linear power law depend upon the cell size L , path-loss factor β , amount of extra information required at each hand over s_h etc., also as in discrete case. For example, higher the path-loss factor and or larger the cell size is, larger is the disparity in the powers allocated to various speed users.

One can easily verify that the continuous power law (18) equals⁸ the limit of the discrete optimal power policy (12). Thus we obtained optimal power law via two different methods for continuous control and the two methods are resulting in the same solution. Also, the optimal power increases linearly with the speed v .

The load factor at optimal power law parametrized by threshold \bar{P} equals:

$$\begin{aligned} \rho^*(L; \bar{P}) &= \frac{\lambda L^2}{K} \int_{V_{min}}^{V_{max}} \left(\frac{C_{\rho,1}}{v} + \frac{C_{\rho,2}}{\bar{P} L^{1-\beta} C_{h,ho} - E[V] \mu s_h} \right) p_V(v) dv \\ &= \frac{\lambda L^2}{K} \left(C_{\rho,1} E\left[\frac{1}{V}\right] + \frac{C_{\rho,2}}{\bar{P} L^{1-\beta} C_{h,ho} - E[V] \mu s_h} \right) \text{ with} \\ C_{\rho,1} &:= C_{b,e} - \frac{C_{b,h} C_{e,ho}}{C_{h,ho}}, \text{ and } C_{\rho,2} := C_{b,h} \left(1 - \mu s_h \frac{C_{e,ho}}{C_{h,ho}} \right). \end{aligned} \quad (19)$$

⁸ As one increases the number of user classes I to infinity, the conditional expectation Y converges to $1/V$ while the sum for any I equals, $\sum_i p_i Y_i = E[1/V]$, the unconditional expectation.

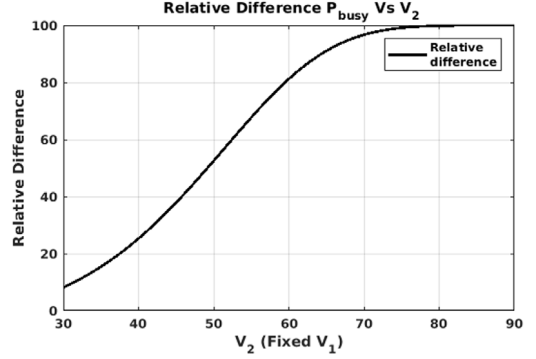


Fig. 5. Relative improvement in P^*_{busy} compared to P_{busy} , as a function of V_2 .

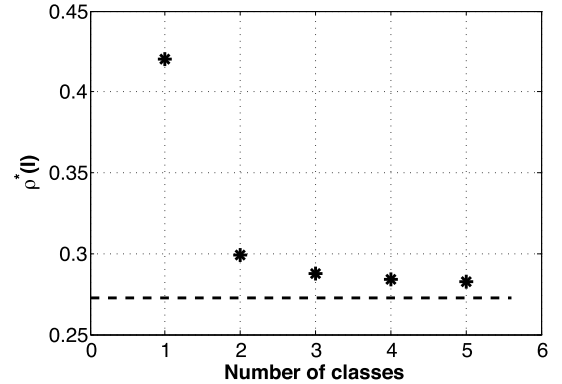


Fig. 6. ρ^* decreases with I and approaches towards the one with continuous law (given by broken line).

5. Numerical examples

We reinforce the theoretical results of previous sections using numerical examples. In the subsequent section, we build an elaborate Monte-Carlo simulation based set-up to study the system with further details.

We first consider a two speed-class example in Fig. 3, with settings as mentioned in caption, and study the differences in the optimal powers allocated to the two sets of users. We consider the equidistant partition of the cell, i.e., $\phi_n = n/N$. We plot the two optimal powers (given by (12)) as a function of path loss factor (β). We notice that the difference between the two allocated powers increases as the path-loss factor increases (see Fig. 3). Thus, power control becomes more important, as the path-loss factor increases.

We study the improvement in load factor and busy probability by using continuous optimal power law in Fig. 4. The parameter settings are as follows: $K = 60$, $N = 9$, $\lambda = 0.7$, $\mu = 0.2$, $s_h = 0.4$, $d_0 =$

10, $\beta = 2.5$, $r_0 = 0.4d_0^{\beta}$, $L = 70$, $\bar{P} = 1.3$. Quantities ρ^* and P_{busy}^* are the performance (ρ given by (15) and P_{Busy} given by (10)) using optimal power law (given by (18)) while ρ and P_{busy} are the performance obtained by allocating equal power to all users (i.e., when $P(v) \equiv \bar{P}$). In Fig. 4, we kept V_1 (V_{min}) fixed at 15 and varied V_2 (V_{max}) from 30 to 90. From the two sub-figures of Fig. 4, it is clear that we obtain significant improvement (upto 60% and 100% respectively) in load factor and P_{Busy} with optimal power law. Further, we calculate percentage relative improvement in P_{Busy} using,

$$\text{Relative difference} = \frac{(P_{busy} - P_{busy}^*)}{(P_{busy} + P_{busy}^*)} \times 200,$$

and plot the same in Fig. 5. We notice a percentage improvement upto 100%. Similar improvements are noted when V_2 is fixed and V_1 is varied.

While conducting the experiments we studied the improvement obtained with finite classes. We notice that the performance with finite classes converges to that of the continuous one and both are close when $I \geq 10$. Thus it appears that one needs fine control (more number of user classes) to obtain good improvement. However, we will observe below that there is a significant jump (Fig. 6) in system performance even with two classes, which further improves as I increases.

Discrete to continuous power law

When one can estimate the speed accurately, one can use finer power control and we expect this to improve the performance significantly. Further one may achieve a major part of this improvement with few classes, as low as 2. This is established in Fig. 6. We compute the load factor ρ , for the case with I number of speed classes, using expression⁹ (15) and when the power law is piece-wise continuous:

$$P(v; I) := \sum_{i \leq I} P_i^*(L; \bar{P}) 1_{\{v \in I_i\}},$$

with constants $\{P_i^*(L; \bar{P})\}_{i \leq I}$ given by (12). The stars in Fig. 6 represent these values for different I . In Fig. 6 we compare these values as I increases, with that obtained using continuous power law (18) (a dashed horizontal line in Fig. 6).

Experimental setting for this figure is same as that in Fig. 4, except for $V_{min} = 20$ and $V_{max} = 90$. We notice that the load factor with optimal power law using finite classes decreases monotonically towards that of the continuous optimal power law. Thus one obtains best performance when one uses the optimal continuous linear power law. However, a significant improvement in performance can be noted for just 2 speed classes (load factor reduces from 0.43 to 0.3) and with $I = 5$ onwards, one can achieve performance very close to the best (0.28).

6. Small cell network simulator

We built a small cell network simulator (SCNS) for elaborate study of the system under consideration. We validate the SCNS before using it for case studies. In all the test cases we compare the performance of the system using proposed linear power law with that of the systems which allocate equal power to all the users. The simulator also enables us to study the test cases that do not satisfy the assumptions required by the theory.¹⁰ In the next section, we consider two such important generalizations.

⁹ As already discussed, with finer divisions, the accuracy of theoretical expressions improve. Hence we use (15) to compute load factor even for discrete case by treating the power law as piece-wise continuous function. With this, the integral of (15) would be replaced by (finite) sum of integrals over sub-intervals.

¹⁰ We proved that the linear power is optimal under certain assumptions (see Theorems 1–2). However we compare an ‘appropriate’ (explained in respective places) linear power allocation strategy with equal power allocation strategy, even for the system configurations/test cases that do not satisfy those assumptions, and found it to perform better.

In all the examples of this section and the next, the pathloss factor β has been set from 2.1 to 3.5. We have also assumed that users are moving with a speed ranging from 20 Kmph to 100 Kmph. The range of the small cells ($2L$) has been set between 140 m to 160 m using a power between 0.7 Watt to 1.6 Watt which corresponds to a typical outdoor metro cell or pico cell.

The SCNS emulates cars moving along a straight road, and receiving services from a series of pico towers adjacent to the road. Without loss of generality, we consider cars moving only in one direction. The SCNS emulates the arrival of new users, service of the user by the nearest tower based on SNR, hand over of services between towers and departure of users from system once service is completed. The simulator also accounts for the data rates lost due to transfer of extra control information per HO. It updates the value of variables at regular time intervals of length δ , where $\delta > 0$ is sufficiently small, to achieve ‘almost’ continuous time simulations. The cars leaving the last tower is tied to the first tower to ensure the stochastic equivalence of cars entering and leaving the system.

Before we proceed, we would like to clarify an important underlying assumption. In SCNS, we assume that there are no transmission errors when one transmits at rates below the SNR/SINR (the approximation for capacity). Here, we are estimating the SNR at any position and then choosing the best rate (among \mathcal{R}) below the SNR. In that sense, these are the results of partial simulations and complete simulations would incorporate channel coding, decoding transmission errors etc. Now, we discuss *several stages* involved in building SCNS.

(1) *Deterministic variables*: A single tower with a single server and a single supported rate is built with all other variables (e.g., inter arrival time, service requests etc.) as deterministic.

(2) *Stochastic variables*: We continued with single tower and single server, but the variables are randomized one by one. We also consider multiple transmission rates. We run simulations for considerably long time to estimate the confidence interval for each case.

(3) *Multiple servers and small cell network*: Finally, we considered the case with multiple towers (each having multiple servers), with the road from final tower leading back to that of the first tower. The performance measures are estimated, after running the simulations for even longer periods to ensure convergence.

6.1. Validation of SCNS

In order to validate our results of the previous sections, we compare the theoretical analysis with simulation results obtained by SCNS. But prior to that, one needs to verify the SCNS itself. Towards this, we build the SCNS in stages, as mentioned above, and some easily computable performance metrics are computed at each stage and are verified against the estimates provided by SCNS. We consider many intermediate measures for this validation purpose. Then, the important performance measures (P_{Busy} and P_{Drop}) are estimated using SCNS and are compared with the theoretical ones.

The results of SCNS are verified using corresponding theoretical expressions first under deterministic setting (when job sizes, user speed etc. are considered constants) and then for stochastic system setting. Then the experiments are performed for small cell network with multiple servers. Theoretical performance measures derived in Section 3 are applicable for this system under following assumptions: (a) the values of $P_{e,ho}$ and $P_{h,ho}$ are close to 1; (b) The values of busy and drop probabilities are small; and (c) The values of V_{min} and V_{max} are away from zero. These assumptions are easily satisfied by almost all practical scenarios (to provide reasonable QoS) and we also consider case studies satisfying these assumptions.

We compare the SCNS based estimates of intermediate performance measures $P_{e,ho}$, $P_{h,ho}$, b_e , b_h with the corresponding theoretical values (given by Eqs. (6), (8), (7)) in Fig. 7. The table details various configurations (Unif meaning uniformly distributed), while the two figures illustrate the comparison of SCNS based estimates with theoretical

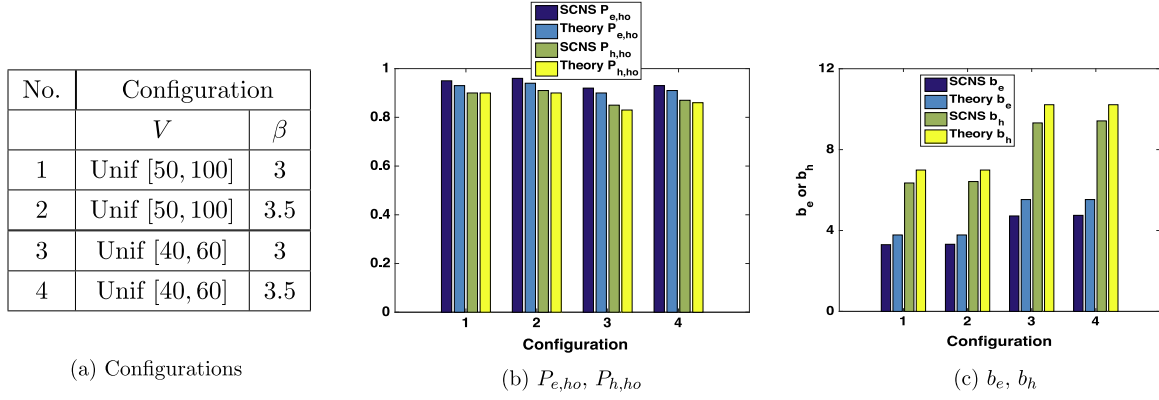


Fig. 7. SCNS based estimates versus theoretical values for different configurations. Other details common to all configurations are $N = 6$, $\phi_n = n/L$, $L = 70$, $d_0 = 10$, $K = 60$, $P = 0.6$, $\mu = 0.22$, $n_{tow} = 7$, $s_h = 0.01$ and $\lambda = 0.7$.

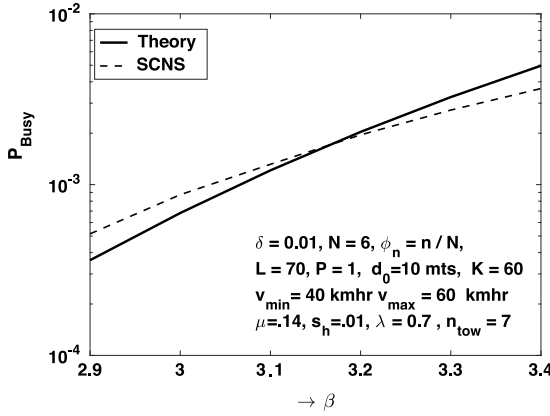


Fig. 8. Theoretical P_{Busy} and its estimate using SCNS.

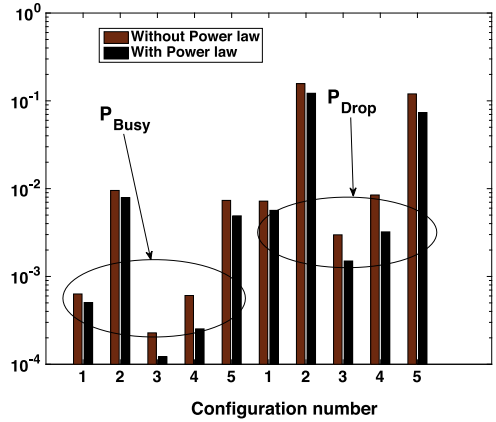


Fig. 9. Performance comparison for different configurations.

Table 1
Test system configurations to compare performance and percentage improvement in performance.

No.	System configurations				P_{Drop} %Improvement
	P	β	s_h	V range	
1	0.85	2	0.4	[20, 30]	24.08
2	1	2.5	0.4	[20, 40]	25.08
3	1.2	2.5	0.4	[20, 25]	66.07
4	1.6	3.1	0.5	[20, 40]	89.82
5	1.6	2.1	0.5	[20, 40]	47.93

expressions. It is clear that there is a good match (around 10 to 15% normalized difference) between the two quantities. Here we define,

$$\frac{200(Per_{th} - Per_{SCNS})}{Per_{th} + Per_{SCNS}}, \quad (20)$$

as the normalized (percentage) difference for any given performance Per .

We complete the final phase of validation, by comparing the blocking probability P_{Busy} estimated using SCNS and its theoretical expression. We consider the case without power law and the results are in Fig. 8, with all system details as given in the figure itself. One can see that there is sufficiently good match in the busy probability performance, with the normalized difference ranging from 2% to 30%. In many more test cases we found similar normalized differences between the performance estimated using SCNS and the theoretical one, as long as the conditions defined at the beginning of this section are satisfied.

6.2. Testing of power law

We now explore the efficiency and optimality of power law. In Section 4, it is theoretically established that affine power law is optimal for small cell network under certain assumptions. We demonstrate the supremacy of the power law, even in scenarios where the system/test case does not satisfy the assumptions required by theory.

Table 1 and Fig. 9 show that power law works well for different (with variety of parameter sets) test cases especially when probability P_{Drop} , P_{Busy} is small (at least of order 10^{-2}). In all test cases the normalized improvement (defined like in (20), now using the estimates with and without power law) is above 24% and for one configuration the improvement is upto 89% (configuration 4 in Table 1). Power law fails when P_{Drop} takes large value in the order of 10^{-1} (see Table 2). The loss in performance due to power law is of orders less than 10%. However, wireless networks generally do not operate in such scenarios due to low efficiency. Thus power law is useful in all ‘operating’ case studies.

Table 3 shows that the performance of power law improves with increase in power (upto 66%). It is noted from the results of Table 4 that the improvement also depends upon the path loss factor β . One has huge improvements for large path-loss scenarios. Further, in all the test cases (irrespective of the configuration), we again notice a very good improvement when P_{Drop} is small and is in the range of 10^{-2} – 10^{-4} (see Tables 3–4). We make a similar observation in the experiments of subsequent section.

We consider another example in Figs. 10–11. We plot the normalized percentage improvement as a function of average power constraint P in Fig. 10, while the block, drop probabilities are plotted in Fig. 11.

Table 2
System configuration (large P_{Drop}) when power law fails.

System configurations				Without power law		With power law		P_{Drop} % improvement
P	β	s_h	V range	P_{Busy}	P_{Drop}	P_{Busy}	P_{Drop}	
1	2.5	0.6	[20, 40]	3.72E-02	6.71E-01	3.90E-02	6.62E-01	-1.35
1	3.1	0.5	[20, 40]	4.05E-02	7.24E-01	4.33E-02	7.40E-01	-2.18

Table 3
Power law performing better for higher power.

System configurations				Without power law		With power law		P_{Drop} % change
P	β	s_h	Range V	P_{Busy}	P_{Drop}	P_{Busy}	P_{Drop}	
1	3	0.4	[20, 40]	2.47E-02	4.30E-01	2.37E-02	3.92E-01	9.24
1.2	3	0.4	[20, 40]	8.25E-03	1.34E-01	6.67E-03	1.02E-01	27.11
1.4	3	0.4	[20, 40]	3.26E-04	4.36E-03	1.75E-04	2.19E-03	66.25

Table 4
Improvement with power law for smaller values of P_{Busy} .

System configurations				Without power law		With power law		P_{Drop} % change
P	β	s_h	Range V	P_{Busy}	P_{Drop}	P_{Busy}	P_{Drop}	
1.6	2.1	0.5	[20, 40]	7.35E-03	1.20E-01	4.90E-03	7.36E-02	47.93
1.6	3.1	0.5	[20, 40]	6.07E-04	8.47E-03	2.53E-04	3.22E-03	89.82

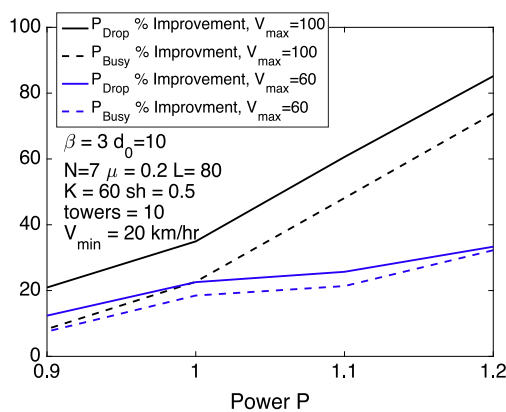


Fig. 10. Normalized % improvement for two cases.

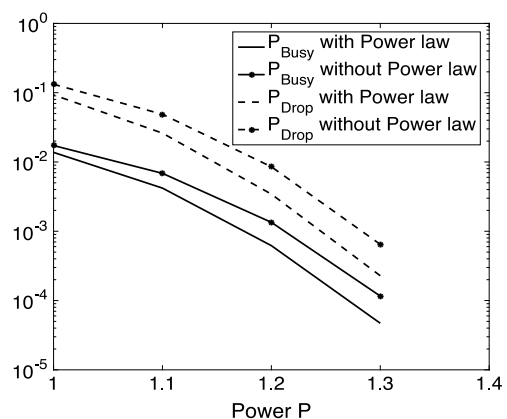


Fig. 11. Block, drop probabilities with and without linear power law, when $V_{max}=100$.

We consider two examples in Fig. 10, the improvement is more when the range of user speeds is larger (black set of curves with $V_{max} = 100$ km/h). From Fig. 11, both drop probability and block probability improve significantly when power law is used (curves without markers are with power law). From theory (Theorems 1–2) the disparity in the powers allocated to different speed classes, increases with increase in the range of user speed, and we observe from both the figures that this increase (in disparity) also increases the normalized improvement obtained using the power law.

7. Numerical illustration: With a common rates set, \mathcal{R} and interference

In previous sections, we assumed that the (finite) set of transmission rate choices \mathcal{R} , depends upon the speed/transmit power of the user. We relax this assumption now and consider a big common set of transmission rate choices. System chooses a rate from the given set based on the received signal strength and rate set is the same for all users. One can choose this common set of possible transmission rates, (\mathcal{R} and N), based on the practical channel coding schemes that would be used in the network design.

We analyse this scenario using the simulator SCNS. We do not have theoretical support as of now for this scenario, however we note that the linear power law can improve the performance. We set power

control rule to be:

$$P(V; \alpha) := \alpha \bar{P} + \bar{P}(1 - \alpha) \frac{V}{E[V]} \text{ for any } \alpha \in [0, 1], \quad (21)$$

and obtain the performance with best α using SCNS. If the set of transmission rates \mathcal{R} is sufficiently big, we found that this rule provides a huge improvement in comparison with the scheme that allocates equal power (i.e., $\alpha = 1$) for all speeds.

The random trajectories of cars moving at random speeds, arriving at random positions with random service requirements is simulated in SCNS. For any given α , the arriving user is allocated a transmit power according to rule (21). As the car moves forward, its position changes and the received power changes accordingly. At any point the best rate among the rates of \mathcal{R} , which is below received SNR (using low SNR approximation (2) for capacity) is chosen as the transmission rate.

We tabulate the improvement in performance with affine power law (21) for many configurations in Table 5, after finding a good $\alpha = 0.7$. We also plot corresponding P_{Busy} , P_{Drop} for all test cases in the adjacent figure, Fig. 12. We notice a significant improvement in performance for all cases. However, this improvement requires the availability of 26 different rate choices as mentioned in the caption of the table. This requirement is mandatory, because using this large set, we can create the effect of significantly different (virtual) cell sizes for different speed classes. In next subsection, we consider an example with common rates set in presence of interference. We notice significant

Table 5

Improvement due to Power Law with common rates set $\mathcal{R} = \{0.8 : -0.035 : 0.03, 0.011 : -0.004 : 0.003\}$ and $|\mathcal{R}| = 26$ Other system parameters: $s_h = 0.4, n = 10, \delta = 0.04, L = 70, V_{min} = 20$ kmph, $V_{max} = 100$ kmph.

Sl. no	System configuration			% Impr
	\bar{P}	β	V range	
1	0.75	3.5	[20, 100]	53
2	0.75	3	[20, 100]	39
1	0.75	2.5	[20, 100]	62
1	0.7	35	[20, 100]	35
1	0.7	3	[20, 100]	29
1	0.7	2.5	[20, 100]	54
1	0.7	3.5	[5, 100]	45
1	0.7	3	[5, 100]	48
1	0.7	2.5	[5, 100]	47

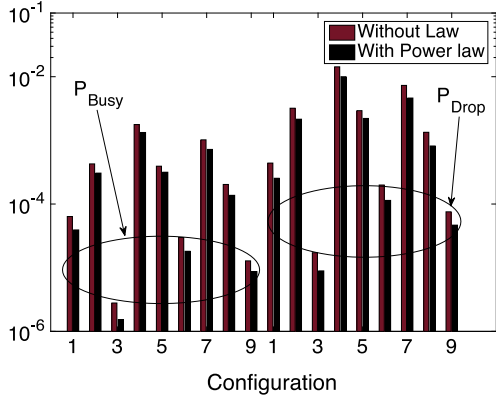


Fig. 12. P_{Busy}, P_{Drop} , with Power law (best $\alpha = 0.7$) and without Power law ($\alpha = 1$).

improvement in this case also (see Fig. 13). Thus by using a big set of transmission rates, we are able to illustrate a very good improvement in performance. It is practically impossible to create different (physical) cell sizes for different speed classes, however one can probably work with a large set of transmission rates. And hence this can be a good design alternative.

7.1. With interference and ‘non-uniform’ speeds

In this subsection, we further consider the effects of interference. Our theoretical results are valid for any distribution of velocity/speed. We also consider speeds that are not uniformly distributed. We assume that the velocity is a conditional Gaussian random variable as below:

$$V = \mathcal{N}\left(\frac{V_{min} + V_{max}}{2}, 10\right) \Big| \mathcal{N} \in [V_{min}, V_{max}],$$

where $\mathcal{N}(m, v)$ is a Gaussian random variable with mean m and variance v . Basically we generate Gaussian random variables and consider only the values that are within $[V_{min}, V_{max}]$. We set $V_{min} = 40$ kmph, $V_{max} = 100$ kmph for this set of experiments. We assume that the towers of the cells other than the serving cell cause interference to the user. The total interference term, I , is computed using the received powers at the user under consideration, received from all the towers that serve the other users currently utilizing the system. These received powers are attenuated values of the power allocated according to rule (21), after distance based attenuation as according to Eq. (3). Hence the interference term and the SINR (Signal to Noise and Interference ratio) of the tagged user equals:

$$I = \sum_{\substack{\text{users of other cells} \\ \text{in same channel}}} P(V_i, \alpha)(d_i/d_0)^{-\beta},$$

$$SINR = \frac{P(V_{tagged}, \alpha)(d_{tagged}/d_0)^{-\beta}}{1 + \frac{I}{\sigma^2}}, \tag{22}$$

where V_i is the velocity of user i , whose tower is at distance d_i from the tagged user and where σ^2 is the thermal noise variance. Recall, by the convention of our paper, that \bar{P} actually represents the transmit power divided by the thermal noise variance. Here, we are estimating the SINR in place of SNR and the best rate (in \mathcal{R}) below the SINR is chosen for transmission, similar to previous section.

Numerical examples

We consider two different case studies and the respective set of (common) rate choices are (respectively of sizes 30 and 45):

$$\mathcal{R}_1 = \{0.83 : -0.03 : 0.01, 0.007, 0.003\},$$

$$\mathcal{R}_2 = \{0.80 : -0.02 : 0.02, 0.009 : -0.002 : 0.001\}.$$

Basically when the path-loss factor is large one requires more number of rate choices.

The results are provided in Fig. 13. This figure has four sub-figures, sub-figure (a) provides the system configuration for all test cases, while the remaining illustrate the performances and the normalized improvement in performance. The light blue bars, orange bars and dark blue bars respectively represent the performance with zero interference, medium interference (noise variance 0.5) and strong interference (noise variance 1) respectively in all the sub-figures. The bars with broken lines as borders represent the performance when linear power law is used. As noted from Fig. 13.(b), the power law improves the performance even for non-uniform speeds. The performance of the system degrades with interference (see sub-figures (c)–(d)), however a significant improvement is noted with power law. We also observe that improvement increases with a bigger set of rates (Configurations 2, 4 and 5 with \mathcal{R}_2). Good α turns out to be smaller for bigger cell sizes (configurations 1 and 2). This indicates a bigger disparity in powers allocated to various speeds.

We considered many more test cases and found that the power law provides good improvement. We noticed that the percentage improvement increases as the SINR increases or equivalently as P_{Drop} decreases.

The percentage improvement is reduced when one considers the effects of interference. Nevertheless the improvement has not diminished completely, but rather is sufficiently significant even with interference. The simulations show an improvement up to 52% (and in many cases well above 9%) even in the presence of (time varying and random) strong interference (dark blue bars of sub-figures of Fig. 13 with $\sigma^2 = 0.1$). In presence of smaller interference (with $\sigma^2 = 0.5$) the percentage improvement is much higher (well above 35% in all cases). Further, the impact of considering interference on reduction in percentage improvement is higher with smaller path losses (first four configurations with $\beta = 2.5$ in Fig. 13).

8. Conclusions

Mobility management is a challenging issue in HetNet deployments, where the main objective is to reduce call drops and network signalling flow, optimize traffic scheduling, and achieve resource optimization. As an example, a common and currently adapted solution for high speed trains is to densify the network along the railway tracks to combat the large penetration loss (coverage holes). However, this will increase HO frequency due to smaller site-to-site distance. Another way is to increase the transmission power of the BSs, which also helps in reducing the large penetration losses. However, this results in high energy consumption (and more interference) and neither of these solutions are cost-effective. Previously in literature, for efficient design, it was suggested to vary inter BS distances based on the speed of the user. However, it is practically infeasible to do so. Alternately, we have proposed in this paper to reflect the speed based (optimal) design variations in the allocated powers.

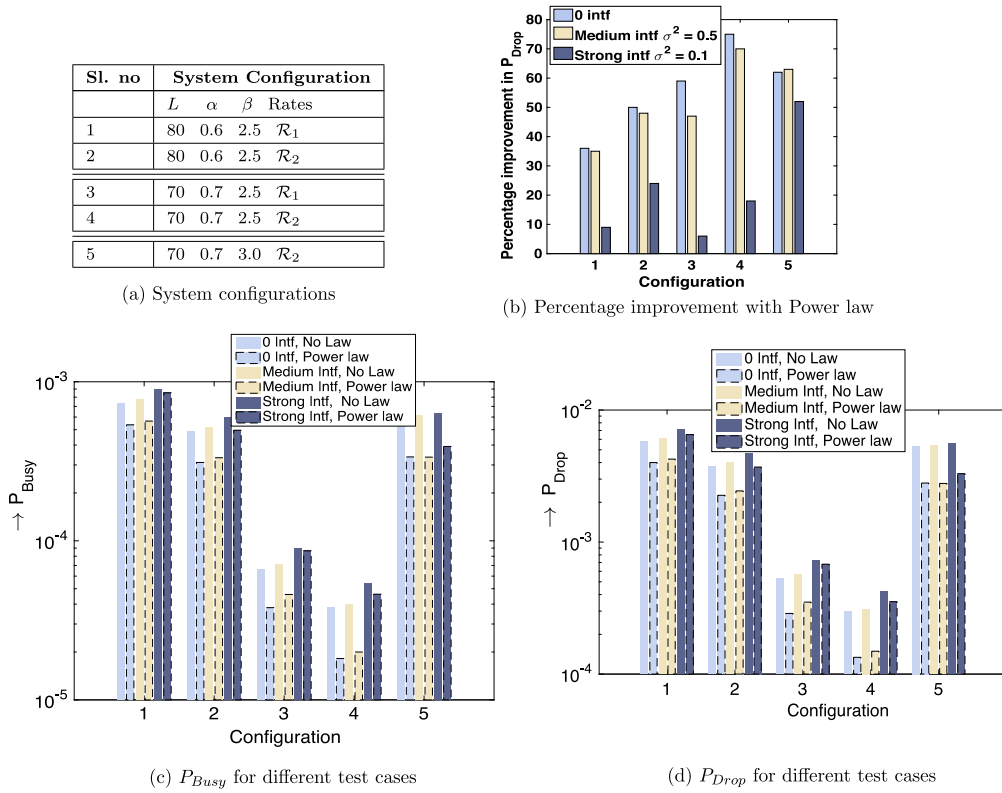


Fig. 13. With interference and ‘non-uniform’ speeds: $\delta = 0.01$, $s_h = 0.4$, $\mu = 0.2$, $K = 60$, $\lambda = 0.7n$, $d_0 = 10$, $\bar{P} = 0.7$ and # of towers $n = 10$ and noise variance $\sigma^2 = 0.5$ (medium interference) or 0.1 (strong interference). From sub-figure (b) % improvement is 50 for the second configuration without considering interference (without interference) while it equals 48 and 24 respectively with noise variances $\sigma^2 = 0.5$ and 0.1. Sub figures (c) and (d) provide P_{Busy} , P_{Drop} respectively, with and without power law, for three levels of interference and for five configurations.

We have obtained a closed form expression for optimal power control (optimal for load factor and/or busy probability), which allocates different transmit powers to different user (speed) classes, for any given average power constraint and the cell size. The optimal control ensures larger power to higher speeds and the differences in the powers allocated increase with path loss factor and the disparities in the speeds. It is noteworthy that whenever an accurate user speed estimate is made available, one can obtain a very fine optimal power control with speed. We have shown that the optimal power varies linearly with the user speed and this result is obtained using Hamilton–Jacobi–Bellman equations.

We have also observed via numerical simulations that, there is large improvement in busy probability and load factor when optimal power control is used instead of equal powers for all users. The improvement in performance increases as the number of user classes increases and one obtains the best improvement with continuous optimal power law. The systems with large (path) losses and or the ones which support wide variations of user speeds, improve significantly with optimal power control.

Further, a system level simulator has been built on which exhaustive simulations were conducted. We have derived the theory under certain assumptions, however the performance of linear power law is estimated using system level simulator for more general set-up. We have observed that power law outperforms the counter part of the systems that uses equal power for all speeds, in all the scenarios with moderate to high SNR conditions. For the system with interference, the power law outperforms by significant margin (even up to 70%) while for systems without interference we noticed an improvement even up to 89% percentage. Achieving these results offers hope that such a smart mechanism can be designed around small cell integration in HetNets. This integration can further help the notion of CSB proposed by LTE standards.

9. Acknowledgement

The authors thank the anonymous reviewers for their useful comments and suggestions that helped in improving of this paper. This work was partially supported by Ministry of Human Resource Development (MHRD), Government of India.

Declaration of competing interest

The authors declare that they have no known competing financial interests or personal relationships that could have appeared to influence the work reported in this paper.

Appendix A. Maximum velocity supported by system

In this section, we calculate a limit on the speeds that can be supported, by a system with maximum N possible transmission rates and with transmission power P . This is equivalent of [8, Theorem 2] obtained for systems with ‘maximal’ transmission rates. User entering at $-L$ when moving with speed V , can transfer in a cell, at maximum (see the discussions while deriving ψ_n given by (4) and using (3))

$$g^N(L) := \frac{L}{NV} \sum_{m=-N}^N r_m = C_{h,ho} \frac{PL^{1-\beta}}{\mu V}, \tag{A.1}$$

bytes of information, out of which s_h are used for HO purposes. So, useful communication is possible only when $g^N(L) > s_h$ with probability one. With $\beta > 1$ (the practical range of path loss factors), $g^N(L)$ reduces with L and so useful communication is not possible for any cell size if $g^N(Nd_0)$ itself is less than s_h and hence we have:

Theorem 3. When $\beta > 1$, there exists a limit on the maximum velocity that can be supported by the system for a given power P

$$V_{lim}(P) := \frac{1}{s_h} r_0 \sum_{n=-N}^N |\phi_n|^{-\beta} P d_0^{1-\beta} N^\beta. \quad \square$$

From the above theorem, given a set of system parameters, useful communication can be achieved by increasing the power P . It is assumed while deriving optimal power law that transmission power P is large enough to ensure useful communication.

Appendix B. Proof of theorem

Proof of Theorem 1. The average power constraint can be satisfied with equality by substituting $P_I = \frac{1}{p_I} (\bar{P} - \sum_{i<I} p_i P_i)$, and then (with $\mathbf{P}_{-I} := (P_1, \dots, P_{I-1})$)

$$\begin{aligned} \rho(L; \bar{P}) &:= \rho \left(L, \left(\mathbf{P}_{-I}, \frac{\bar{P} - \sum_{i<I} p_i P_i}{p_I} \right) \right) \\ &= \frac{\lambda L^2}{K} \sum_{i<I} p_i Y_i \left(C_{b,e} + C_{b,h} \frac{1 - \delta_i C_{e,ho}}{\delta_i C_{h,ho} - \mu s_h} \right) \\ &\quad + \frac{\lambda L^2}{K} p_I Y_I \left(C_{b,e} + C_{b,h} \frac{1 - \bar{\delta}(\mathbf{P}_{-I}) C_{e,ho}}{\bar{\delta}(\mathbf{P}_{-I}) C_{h,ho} - \mu s_h} \right), \\ \bar{\delta}(\mathbf{P}_{-I}) &:= \frac{1}{p_I} \left(\bar{P} - \sum_{i<I} p_i P_i \right) Y_I L^{1-\beta}. \end{aligned}$$

We obtain the optimizer of the load factor ρ via the zeros of the derivatives (if they exist). The partial derivatives (for all $i < I$) are given by:

$$\begin{aligned} \frac{d\rho}{dP_i} &= \frac{\lambda}{K} C_{b,h} p_i Y_i^2 L^{3-\beta} \frac{C_{e,ho} \mu s_h - C_{h,ho}}{(\delta_i C_{h,ho} - \mu s_h)^2} \\ &\quad - \frac{\lambda}{K} C_{b,h} p_i Y_i^2 L^{3-\beta} \frac{C_{e,ho} \mu s_h - C_{h,ho}}{(\bar{\delta}(\mathbf{P}_{-I}) C_{h,ho} - \mu s_h)^2} \\ &= \frac{\lambda}{K} C_{b,h} p_i L^{3-\beta} (C_{e,ho} \mu s_h - C_{h,ho}) \\ &\quad \times \left(\frac{Y_i^2}{(\delta_i C_{h,ho} - \mu s_h)^2} - \frac{Y_I^2}{(\bar{\delta}(\mathbf{P}_{-I}) C_{h,ho} - \mu s_h)^2} \right). \end{aligned} \quad (\text{B.1})$$

One can easily obtain the zero of Eq. (B.1), i.e., the equilibrium point. Equating the partial derivatives to zero, $\partial\rho/\partial P_i = 0$ for all i , the optimal power control $\mathbf{P}(L, \bar{P})$, for a given cell size and average power constraint \bar{P} equals:

$$\begin{aligned} \mathbf{P}^*(L) &= \begin{bmatrix} -1 & 0 & 0 & \dots & 0 & 1 \\ 0 & -1 & 0 & \dots & 0 & 1 \\ & & \vdots & & & \\ 0 & 0 & 0 & \dots & -1 & 1 \\ p_1 & p_2 & p_3 & \dots & p_{I-1} & p_I \end{bmatrix}^{-1} \frac{\mu s_h L^{\beta-1}}{Y_I C_{h,ho}} \mathbf{v}_\mu \\ \mathbf{v}_\mu &:= \left[\frac{Y_1 - Y_I}{Y_1}, \frac{Y_2 - Y_I}{Y_2}, \dots, \frac{Y_{I-1} - Y_I}{Y_{I-1}}, \bar{P} \right]. \end{aligned} \quad (\text{B.2})$$

This can be solved easily and

$$P_i^*(L; \bar{P}) = \bar{P} + \frac{\mu s_h L^{\beta-1}}{C_{h,ho}} \sum_{j<I} p_j \left(\frac{1}{Y_I} - \frac{1}{Y_j} \right) - \frac{\mu s_h L^{\beta-1}}{C_{h,ho}} \left(\frac{1}{Y_I} - \frac{1}{Y_I} \right).$$

This simplifies to (12). Differentiating (B.1) again, the Hessian matrix equals:

$$\frac{2C_{h,ho} \lambda C_{b,h} L^{4-2\beta} (C_{h,ho} - C_{e,ho} \mu s_h) Y_I^3}{K (\bar{\delta}(\mathbf{P}_{-I}) C_{h,ho} - \mu s_h)^3} P_V,$$

where P_V is defined in the hypothesis of the theorem. This is a positive definite matrix under the given assumptions and hence \mathbf{P}^* given by (12) is indeed a minimizer. \square

Appendix C. Expected overall service time B

Let $Z = (H_O, V)$ represent a joint random variable in which the first component is an indicator that it is due to HO, i.e., $H_O = 1$ implies it is an HO call. The following are the events given that a call has arrived. We first consider HO case. Let \check{V} and \check{H}_O represent the velocity and the call type (HO or external) in the previous cell before the Handover to the current cell. That is, $\check{H}_O = 1$ implies it was a HO call in the previous cell and is again handed over to the current cell. For any set \mathcal{A} , since the velocity of user remains constant during the call:

$$\begin{aligned} P(H_O = 1, V \in \mathcal{A}) &= P(H_O = 1, \check{V} \in \mathcal{A}) = P(H_O = 1, \check{V} \in \mathcal{A}, \check{H}_O = 0) \\ &\quad + P(H_O = 1, \check{V} \in \mathcal{A}, \check{H}_O = 1) \end{aligned} \quad (\text{C.1})$$

By stationarity $P(\check{H}_O = 0) = P(H_O = 0)$ and this equals the probability that a call arrived is a new call. By ergodicity this equals λ_L/λ . Thus, by conditioning first on \check{H}_O and then on \check{V} we obtain:

$$\begin{aligned} P(H_O = 1, \check{V} \in \mathcal{A}, \check{H}_O = 0) &= P(H_O = 1, \check{V} \in \mathcal{A} | \check{H}_O = 0) P(\check{H}_O = 0) \\ &= \int_{\mathcal{A}} P_{e,ho}(v) p_V(v) dv \frac{\lambda_L}{\lambda}. \end{aligned} \quad (\text{C.2})$$

Considering infinitesimal interval $vdv := [v - dv, v + dv]$ and conditioning as in the previous equation we obtain:

$$\begin{aligned} P(H_O = 1, \check{V} \in vdv, \check{H}_O = 1) &= P(H_O = 1 | \check{V} \in vdv, \check{H}_O = 1) P(\check{H}_O = 1, \check{V} \in vdv) \\ &\approx P_{h,ho}(v) P(\check{H}_O = 1, \check{V} \in vdv). \end{aligned} \quad (\text{C.3})$$

By stationarity (and S being memoryless), $P(\check{H}_O = 1, \check{V} \in vdv) = P(H_O = 1, V \in vdv)$ and thus by substituting (C.2), (C.3) into (C.1),

$$P(H_O = 1, V \in vdv) \approx \frac{P_{e,ho}(v) p_V(v) dv \lambda_L}{1 - P_{h,ho}} \frac{1}{\lambda}. \quad (\text{C.4})$$

In a similar way,

$$\begin{aligned} P(H_O = 0, V \in vdv) &= P(V \in vdv | H_O = 0) \frac{\lambda_L}{\lambda} \\ &\approx p_V(v) dv \frac{\lambda_L}{\lambda}. \end{aligned} \quad (\text{C.5})$$

Note that service requirements S is independent of $Z = (H_O, V)$. Hence, using Eq. (13) and Eqs. (C.1)–(C.5) and conditioning on Z , the average of the overall service time equals Eq. (14).

References

- [1] Cisco Visual Networking Index: Global Mobile Data Traffic Forecast Update, 2015–2020 (White Paper), Cisco Systems, 2016.
- [2] Qualcomm, The 1000x mobile data challenge: More small cells, more spectrum, higher efficiency, Nov. 2013.
- [3] D.L. Perez, I. Guvenc, X. Chu, Mobility management challenges in 3GPP heterogeneous networks, *IEEE Commun. Mag.* 50 (12) (2012) 70–78.
- [4] Nokia Outdoor 3G/LTE Small Cells Deployment Strategy: The Race to the Pole, Nokia Whitepaper, available at <http://networks.nokia.com/file/30711/outdoor-3glte-small-cells-deployment-strategy-the-race-to-the-pole>.
- [5] J. Andrews, Seven ways that hetnets are a cellular paradigm shift, *IEEE Commun. Mag.* 51 (3) (2013) 136–144.
- [6] Beyond the base station router, Alcatel-Lucent technical note available at <http://innovationdays.alcatel-lucent.com/2008/documents/Beyond%20BSR.pdf>.
- [7] D.G. Herculua, C.S. Chen, M. Haddad, V. Capdevielle, STRAIGHT: Stochastic geometry and user history based mobility estimation, in: HotPOST held in conjunction with the 17th ACM MobiHoc, May 2016.
- [8] V. Kavitha, S. Ramanath, E. Altman, Spatial queueing for analysis, design and dimensioning of picocell networks with mobile users, *Perform. Eval.* (2011).
- [9] V. Capdevielle, S. Ramanath, E. Altman, R. Roullet, Cell Partitioning for High speed users, Case 809154-EP-EPA.
- [10] M. Haddad, V. Capdevielle, A. Feki, E. Altman, Method and system for user speed estimation in wireless networks, Filed patent 813871-EP-EPA, March 2013.
- [11] A. Merwady, I. Guvenc, W. Saad, A. Mehdodniya, F. Adachi, Sojourn time-based velocity estimation in small cell Poisson networks, *IEEE Commun. Lett.* 20 (2) (2016) 340–343.

- [12] M. Haddad, D.-G. Herculea, C.S. Chen, E. Altman, V. Capdevielle, Online Mobile User Speed Estimation: Performance and Tradeoff Considerations, in: IEEE CCNC, Las Vegas, USA, Sept. 2016.
- [13] M. Chiang, P. Hande, T. Lan, C.W. Tan, *Power Control in Wireless Cellular Networks*, Now publishers, 2008.
- [14] G.J. Foschini, Z. Miljanic, A simple distributed autonomous power control algorithm and its convergence, *IEEE Trans. Veh. Technol.* 42 (4) (1993).
- [15] C. Wu, D.P. Bertsekas, Distributed Power Control Algorithms for Wireless Networks, *IEEE VTC*, 2001.
- [16] T. Holliday, A. Goldsmith, P. Glynn, N. Bambos, Distributed power and admission control for time varying wireless networks, *Globecom*, Nov 2004.
- [17] S. Ulukus, R. Yates, Stochastic power control for cellular radio systems, *IEEE Trans. Commun.* 46 (6) (1998) 784–798.
- [18] R.D. Yates, A framework for uplink power control in cellular radio systems, *IEEE J. Selected Areas Commun.* 13 (7) (1995) 1341–1347.
- [19] T. ElBatt, A. Ephremides, Joint scheduling and power control for wireless ad hoc networks, *IEEE Trans. Wireless Commun.* 3 (1) (2004) 74–85.
- [20] M. Andersin, Z. Rosberg, Time variant power control in cellular networks, in: *Proc. PIMRC*, 1996, pp. 193–197.
- [21] R. Patachaian, K. Sundrasegaran, An Adaptive step size power control with transmit power control command aided mobility estimation, in: *Proceedings of IASTED Asian Conference, Communication Systems and Networks*, 2007.
- [22] H. Lee, D.H. Cho, A new user mobility based adaptive power control in CDMA systems, *IEICE Trans. Commun.* E86-B (5) (2003).
- [23] V. Kavitha, V. Capdevielle, M.K. Gupta, Small cell networks: speed based power allocation, in: *Communication, Control, and Computing (Allerton)*, 2013 51st Annual Allerton Conference on, IEEE, 2013.
- [24] Philip V. Orlik, Stephen S. Rappaport, On the handoff arrival process in cellular communications, *Wirel. Netw.* (2001).
- [25] S. Dharmaraja, Kishor S. Trivedi, Dimitris Logothetis, Performance analysis of cellular networks with generally distributed handoff interarrival times, *Comput. Commun.* (2003).
- [26] V. Kavitha, S. Ramanath, E. Altman, Analysis of Small Cells with Randomly wandering Users, *WiOpt 2012* Longer version of the paper at <http://hal.inria.fr/hal-00660647>.
- [27] T. Başar, G.J. Olsder, *Dynamic Noncooperative Game Theory*, in: *SIAM Series in Classics in Applied Mathematics*, Philadelphia, 1999.
- [28] W.H. Fleming, R.W. Rishel, *Deterministic and Stochastic Optimal Control*, Springer-Verlag, 1975.